Two absolute integral measurements of the ^{197}Au(n,γ) stellar cross-section and solution of the historic discrepancies.

Javier Praena[1*] and *Pablo* Jiménez-Bonilla[2]

[1]Atomic, Molecular and Nuclear Physics Department, University of Granada, Spain.
[2]Atomic, Molecular and Nuclear Physics Department, University of Seville, Spain.

Abstract. The Maxwellian averaged cross section (MACS) for ^{197}Au(n,γ) is used in neutron capture cross section measurements as a reference for reactions important for astrophysics, reactor and dosimetry applications. The traditionally adopted value for this reference cross section, in the energy range relevant for astrophysical ($3 < E_n < 200$ keV), was obtained by Ratynski and Käppeler in 1988. However, the MACS calculated using the 2006 standards evaluation is approximately 6 % above the Ratynski and Käppeler (R&K) evaluation. Because of this discrepancy new experiments and reanalyses were done in an attempt to resolve the problem. In 2011 we started as well a series of integral experiments (activation) for determining the MACS-30 (kT=30 keV) of Au with two different Maxwellian neutron spectra: i) QMNS-25 (as R&K) and ii) MNS-30 (new method). Our results agree with those obtained with the standard evaluation. At present (2018), the updated MACS-30 has been included as standard. Here we present the results of our measurements and the reasons for the lower value of the R&K measurement.

1 Introduction

Most neutron cross section measurements are made relative to the neutron cross section standards. ^{197}Au(n,γ) is the only capture cross section standard. In 2007 standards evaluation, ^{197}Au(n,γ) cross-section was considered a standard at 0.0253 eV and at the 0.2-2.5 MeV energy range [1]. Moreover, the Maxwellian averaged cross section (MACS) for ^{197}Au(n,γ) is used in neutron capture cross section measurements as a reference for reactions important for astrophysics, reactor and dosimetry applications.

In the helium-burning phase in red giants stars, neutrons are produced via (α,n) reactions. Neutron capture processes (s-process and r-process) are responsible for the nucleosynthesis of the main part of the heavy elements beyond iron [2]. Neutrons inside the stars are quickly thermalized through elastic scattering, and the velocity probability distribution is represented by a Maxwell-Boltzmann distribution. The maximum probability corresponds to the T of the medium (thermal energy kT). In astrophysics, kT depends on the mass and evolutionary stage of the star, and the MACS is specially of interest for kT=5, 30, 90 keV. The MACS is defined as the ratio between $\langle\sigma v\rangle$ (reaction rate per particle pair) and v_T (particle most probably thermal velocity for a temperature T). Its expression is showed in eq. 1.

$$MACS \equiv \langle\sigma\rangle = \frac{2}{\sqrt{\pi}} \cdot \frac{1}{(kT)^2} \cdot \int_0^\infty \sigma(E) \cdot E \cdot e^{-\frac{E}{kT}} dE \qquad (1)$$

The MACS can be calculated analytically at any kT if the neutron-capture cross-section, measured as a function of the energy (i.e. using time-of-flight technique) is known. However, as shown by Beer & Käppeler [3], MACS at kT≈25 keV can be measured almost directly for many isotopes using activation technique. In this method, a quasi-Maxwellian neutron spectrum (QMNS) is generated using the ^{7}Li(p,n)^{7}Be reaction. Later, the best approach to a Maxwell spectrum was achieved by Ratynski and Käppeler when the proton energy was adjusted to Ep=1912 keV [4]. With the criterion of overlapping of areas the optimal kT was selected equal to 25 keV. After irradiating the sample, if the nucleus produced by the neutron capture reaction is radioactive (with a convenient half-life), the subsequent gamma activity measurement will allows us to obtain the experimental neutron capture cross section. This experimental cross section is then a quasi-Maxwellian averaged cross section, and this value must be corrected later, taking into account the different between the quasi-maxwellian spectrum and a true stellar maxwellian one. In addition to this, if the MACS at kT=30 keV or other energies is needed an extrapolation from 25 to 30 keV is necessary. For both, correction and extrapolation, the knowledge or assumption of the cross-section as a function of the energy is mandatory. This activation method has been extensively used for MACS measurements of many isotopes relevant to the s-process.

A temperature of $T=348 \cdot 10^6$ K, typical of helium-burning in red giants stars, corresponds to an energy of kT=30 keV. The MACS of ^{197}Au(n,γ) at kT=30 keV is

* Corresponding author: jpraena@ugr.es

used as a reference, and the traditionally adopted value for the MACS-30 was obtained by Ratynski & Käppeler, in an accurate activation measurement using a spherical segment gold sample [4]. They reported a value equal to (582±9) mb. However, more recent evaluations performed in different data base show values 6% above this measurement [1]. Because of this discrepancy new experiments and reanalyses were done in an attempt to resolve the problem. Measurements in 2011 of the ^{197}Au(n,γ) cross section with the time-of-flight (TOF) technique at n_TOF facility at CERN reported a value of (611±22) mb [6], and similar value (613±9 mb) at TOF facility at Gelina [7] in 2014.

In 2011 we started as well a series of integral measurements (activation experiments) for determining the MACS-30 of Au with two different Maxwellian neutron spectra: i) with QMNS-25 (as Ratynski & Käppeler) and ii) with an improved neutron spectrum (MNS-30). Our first results, reported in [8,9], agreed with the standard evaluation and TOF experiments.

MACS-30 was updated to a value of 613±7 mb in the astrophysical database Kadonis v1.0 [10] in 2017, and more recently this MACS-30 has been included as a standard in the last standard evaluation in 2018 [11], with a value of 620±11 mbarn.

2 Experimental setup.

Both activation experiments were carried out at the 3MV Tandem Pelletron accelerator at CNA (Seville). For the first activation (QMNS), the proton energy was adjusted to Ep=1912 keV. The accelerator terminal and the 90º analyzing magnet were carefully calibrated before the experiment, using the 991.86 keV ^{27}Al(p,γ)^{28}Si and 2409 keV ^{24}Mg(p,p'γ)^{24}Mg resonances, and with the Rutherford backscattering technique for alpha beam of higher terminal voltages. The energy spread for proton beam at these energies was less than 1 keV.

The setup consisted of a copper backing that held the metallic lithium target and the gold sample. The dimensions of the backing were 3x3x0.8 cm^3 with a centered cylinder hole of 1 cm in diameter and 0.75 cm in height to place the thick lithium layer (of 120 µm thickness). The backing contains an internal cooling water circuit (centered toroid). The gold sample, 2.5cm diameter and 0.1mm thickness, was secured to the back surface of the backing. The copper backing between the lithium layer and the gold sample was 0.5 mm thickness. At the proton beam energy of the experiment, E_p=1912 keV, all the neutrons produced by the ^{7}Li(p,n) reaction are kinematically collimated into a forward cone of about 140º opening angle. So, except for scattered neutrons at high angles, the entire neutron flux is completely impinging on the gold sample. Metallic lithium reacts both with nitrogen and oxygen at room temperature. Therefore, the lithium foil was always stored and manipulated in inert gas to avoid its degradation. Neutron irradiation time was 4 h 45 min. During the irradiation, neutron dosimetry and proton current on the target was recorded in order to correct possible beam instabilities. The produced ^{7}Be and ^{198}Au have a half-life of 53,29 and 2,6947 days respectively. After the irradiation, a HPGe Ortec GMX gamma detector was placed at 28 mm distance from the backing, in order to measure the gamma-rays lines of 477,6 keV and 411,8 keV emitted in the decay of the beryllium and gold, respectively. Activity was measured during 6 h 30 min. Time between end of irradiation and beginning of activity measurement was 15 min.

For the second activation, a similar setup was used, but with an improved method for the production of Maxwellian Neutron Spectra (MNS), closer than QMNS to a real maxwellian one. The method is based on the shaping of the proton beam to a Gaussian-like distribution (GPD), introducing a foil degrader upstream of the lithium target. This method was proposed in [12] and checked in [13,14]. Different combinations of proton energy and degrader material and thickness are suitable for generating Maxwellian-30. The GPDs were measured [13] and neutron spectra were obtained by means of analytical descriptions of the differential neutron yield in angle and energy of the ^{7}Li(p,n) reaction and Monte Carlo (MC) simulations of the neutron transport through the experimental setup (SIMPRO procedure) [13,14]. We used the setup described in [13], with a proton beam energy of 3.7 MeV and the Al degrader 75 µm in thickness. Irradiation time was 210 min and measured time was 13h.

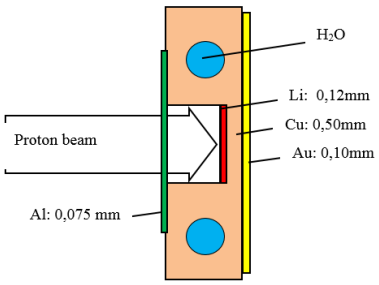

Figure 1: Scheme of Li target, Au sample and Cu backing used in the activations (and Al foil for the MNS case).

3 Data analysis.

The cross section can be deduced if the number of activated nuclei A, the neutron fluence through the sample Φ, and the sample mass thickness N are known (eq. 2).

$$\sigma_{exp} = \frac{1}{N_{Au}} \cdot \frac{A_{Au}}{\Phi} \qquad (2)$$

A, the number of activated nuclei, can be determined from the γ-ray spectra measured with the HPGe detector. In eq. 3, C is this number of events registered by the detector:

$$\sigma_{exp} = \frac{1}{N_{Au}} \cdot \frac{C_{Au}}{C_{Be}} \cdot \frac{[f_d \cdot I_\gamma \cdot \varepsilon \cdot k_\gamma]_{Be}}{[f_d \cdot I_\gamma \cdot \varepsilon \cdot k_\gamma]_{Au}} \cdot \frac{1}{k_s} \cdot \frac{1}{k_f} \qquad (3)$$

I_γ is the gamma intensity of the 477,6 keV and 411,8 keV lines, corresponding to 10,44% and 95,54% respectively; ε is the HPGe gamma detector efficiency (including energy efficiency and geometric efficiency that takes into account the extended samples effects); k_γ is the correction due to the gamma absorption and scattering in materials, before the gammas reach the detector (and total efficiency $\varepsilon = \varepsilon \cdot k_\gamma$); k_s reflects the neutron scattering (mainly due to Cu backing but also due to the sample); k_f is a correction due to the flat sample used in our experiment: it must be noticed that the Au sample thickness as seeing by neutrons passing through Au depends on the entering angle θ inside the sample. Ratynski & Käppeler used a semi-spherical sample to appear equally thick to all neutrons [4].

The factor f_d relates the number of the decay nuclei during the measurement time (t_m) with the total number of activated nucleus (during irradiation time, t_a). It also includes the decay nuclei during the waiting time (t_w), thus the time between the end of neutron irradiation and the beginning of activity measurement with the HPGe detector, and ϕ(t) is the neutron flux (eq. 4).

$$f_d = \frac{e^{-\lambda t_a} \cdot \left(\int_0^{t_a} \phi(\tau) \cdot e^{\lambda \tau} d\tau\right)}{\int_0^{t_a} \phi(\tau) \cdot d\tau} \cdot \left(e^{-\lambda t_w}\right) \cdot \left(1 - e^{-\lambda t_m}\right) \quad (4)$$

C_{Au} and C_{Be} were counted using Canberra GENIE2000 software connected to the acquisition system consisting of HPGe, a high voltage supply HVPS 9645 Canberra and digital signal processor DSP 9660 Canberra. Mass thickness N_{Au} was obtained with accurate measurements of mass (0.3820 g) and surface (206,12 mm^2) of the gold sample, cutting the gold sample after irradiation for a more precise measurement of the activated region. The curve of the gamma energy efficiency of the HPGe was first experimentally calculated using calibrated point sources. Then, a series of MCNPX simulations for those point sources and the HPGe detector were carried out, adjusting the geometry and dead layer thickness of the germanium crystal from its nominal value provided by the manufacturer to a value that fits better with the experimental point sources efficiency. This allowed getting a more reliable modelling of the HPGe for a subsequent full MCNPX simulation (fig. 2) to calculate the gamma efficiency.

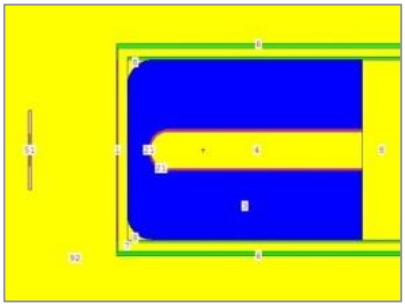

Figure 2: MCNPX simulation of the setup for activation measurement (target and HPGe detector).

For the k_s calculation, a Fortran code [12] was used to generate the energy-angle distribution of the neutrons for the ^{7}Li(p,n) reaction, as the input for MCNPX. The code and the MCNPX simulations for the proton energy (1912 keV) involved in this experiment were tested with experimental data, see details in [13]. For k_f calculation, the angle-energy distribution of the neutron spectrum ϕ(θ,E) and the energy dependence of the ^{197}Au(n,γ) cross section must be taken into account. We proposed in [8] an analytical expression for k_f. However, these two corrections k_s and k_f are coupled (the scattering increases the effective angular aperture, as seen in fig. 3 left), so it is more effective to calculate at the same time the neutron scattering correction and the flat sample correction with MCNP simulations, in a single k_n correction. We obtained this k_n correction comparing detailed simulations of the real activation experiment (angle aperture and scattering, fig. 3 left) with an ideal activation situation (zero angle aperture and no scattering, fig.3 right).

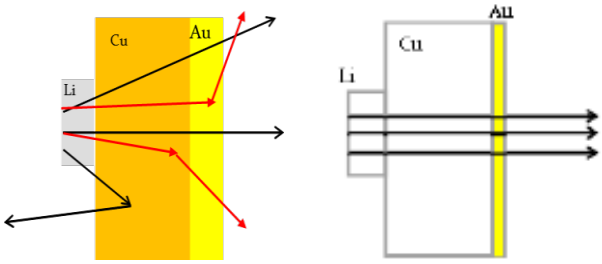

Figure 3: Left: scheme of some possible neutron scattering effects in a real experiment. Right: ideal activation experiment.

We analysed the data of the QMNS experiment in that way, obtaining k_n = 1,28. In the case of MNS method the aperture of the neutron cone is larger than in QMNS at 1912 keV, then, the correction due to flat sample and neutron scattering will become more important, obtaining k_n = 1,75. It has to be notice that this correction also depend on the σ(E) of the element, so it has to be calculate for the specific element of the sample, and as we pointed out in [15] it could be important even in relative measurements, where historically it hasn't been taken into account.

Finally, in order to obtain the MACS, we need to correct our experimental cross-section (σ_{exp}), due to the difference between a quasi-maxwellian neutron spectrum and a true maxwellian neutron spectrum at kT=25 keV y kT=30 keV. To perform the calculation of this correction (factor k_{max}), it is needed the experimental neutron spectrum and the energy-dependence of the cross-section $\sigma(E)$. In the case of MNS, the correction is only about 1%.

$$MACS = \frac{2}{\sqrt{\pi}} \cdot k_{max} \cdot \sigma_{exp} \quad (5)$$

$$k_{max} = \frac{\int_0^\infty \sigma(E)\cdot E\cdot e^{-\frac{E}{kT}}dE \Big/ \int_0^\infty E\cdot e^{-\frac{E}{kT}}dE}{\int_0^\infty \sigma(E)\cdot \phi(E)dE \Big/ \int_0^\infty \phi(E)dE} \quad (6)$$

We resume the experimental data and obtained corrections and MACS in table 1.

Table 1. Experimental data, obtained corrections and MACS.

	QMNS	**Unc. (%)**	**MNS**	**Unc. (%)**
$I_{\gamma Be}$	0,1045	0,04	0,1045	0,04
$I_{\gamma Au}$	0,9554	0,07	0,9554	0,07
N_{Au}	5,67E-4	1,5	6,37E-4	1,5
C_{Be}	332000	0,3	546000	0,3
C_{Au}	32950	0,7	64100	0,7
f_{dBe}	0,00352	0,1	0,00706	0,1
f_{dAu}	0,06545	0,01	0,12818	0,01
$\epsilon_{\gamma Be}/\epsilon_{\gamma Au}$	0,80	2	0,80	2
k_n	1,28	1	1,75	1,5
k_{MACS25}	0,95	1,4	-	-
k_{MACS30}	0,86	1,5	1,01	1,5
MACS-30	**626±25 mb**	3,5	**612±21 mb**	3,5

3 Results and conclusions.

We obtained a value of MACS of ^{197}Au(n,γ) at kT=30 keV of 621 mb in our first activation experiment with QMNS method, and a value of 612 mb in our second experiment with MNS method. As seen in table 2, these two values are in good agreement with the latest evaluations.

Table 2. Comparison of MACS values of ^{197}Au(n,γ) at kT=30 keV.

Authors	**Method Sample Spectrum**	**MACS at 30 keV (mbarn)**
Ratynski & Käppeler [4]	Activation Spherical QMNS-25	582 ± 9
This work [8]	Activation Flat QMNS-25	626 ± 25
This work [9]	Activation Flat sample MNS-30	612 ± 21
Kadonis (2017)	Evaluation	613 ± 7
Evaluation of the Neutron Data Standards (2018)	Evaluation	620 ± 11

Looking for a possible explanation of the lower R&K value, we simulated in MCNX the R&K setup, with a 1 mm Cu backing, and we found that in that case the simulation indicates a 5% of neutron loss due to scattering. However, R&K estimated experimentally only a 1.8% of scattering. A second factor could be the half-life taken for the ^{198}Au. In that paper R&K indicated 2,62 d, and the accepted value at present is 2,69 d, which means a 10 mb difference in the MACS calculation. A third factor, to be studied is the neutron range considered (above 3 keV) for the spectrum correction by R&K. It should be noticed that the correction increases with the ^{197}Au(n,γ) cross-section for lower energies and also because the authors claimed that neutrons down to 1 keV were detected [4].

Acknowlegments.
This work has been supported by the Spanish projects FIS2015-69941-C2-1-P and FPA2016-77689-C2-1-R, (MINECO-FEDER,EU),A-FQM-371-UGR18 (Programa Operativo FEDER Andalucia 2014-2020), and the Spanish Association Against Cancer (AECC) (Grant No. PS16163811PORR).

References

[1] A.D. Carlson *et al.*, Nucl. Data Sheets 110, 12, 3215-3324, (2009).

[2] E. M. Burbidge, G. R. Burbidge, W. A. Fowler, F. Hoyle, Rev. Mod. Phys., vol. 29, nº 4, pp. 547-650, (1957).

[3] H. Beer, F. Käppeler. Phys. Rev. C, vol. 21, nº 2, p.534–544 (1980).

[4] W. Ratynski, F. Käppeler, Phys. Rev. C, 37 (1988).

[5] M. Chadwick *et al.*, Nucl. Data Sheets 112, 2887 (2011).

[6] C. Lederer *et al.*, (n_TOF collaboration), Phys. Rev. C, vol. 83, nº 034608, (2011).

[7] Massimi *et al.*, Eur. Phys. J. A, 50: 124, (2014).

[8] P. Jiménez-Bonilla and J. Praena. Proceedings of Science PoS (NIC XIII Conf.) 102 (2014).

[9] P. Jiménez-Bonilla, J. Praena, J.M. Quesada, NPA VII Conf., J. Phys.: Conf. Ser. 940 012044 (2018).

[10] I. Dillmann, R. Plag, F. Käppeler, *et al.*, PoS (NIC XIII Conf.) 057 (2014).

[11] A.D. Carlson, V.G. Pronyaev, R. Capote *et al.*, 2018. Nuclear Data Sheets 140, 143-188.

[12] P. F. Mastinu, G. Martín-Hernández and J. Praena. Nucl. Inst. and Meth. A 601, 333-338 (2009).

[13] J. Praena, P.F. Mastinu, M. Pignatari *et al.,* Nucl. Inst. and Meth. A, 727 1-6 (2013).

[14] J. Praena, P.F. Mastinu, R. Capote *et al.,* Nuc. Data Sheets 120, 205–207 (2014).

[15] P. Jiménez-Bonilla, J. Praena, J.M. Quesada, NIC XV Conf. (2018), Springer Proceedings in Physics 219, https://doi.org/10.1007/978-3-030-13876-9_70.